JOURNAL OF MATERIALS SCIENCE 27 (1992) 4300–4304

Carbothermal synthesis of titanium nitride

Part III *Kinetics and mechanism*

G. V. WHITE, K. J. D. MACKENZIE, I. W. M. BROWN
DSIR Chemistry, Private Bag, Petone, New Zealand
J. H. JOHNSTON
Chemistry Department, Victoria University of Wellington, New Zealand

The growth curves for TiN formed from four anatases and two rutiles by carbothermal reduction in nitrogen at 1090–1230 °C were analysed in terms of several different mathematical models. The results for all samples over the complete temperature range are best described by first-order kinetics. Arrhenius plots show evidence of two lines intersecting at about 1100 °C. Above this temperature, the activation enthalpies for the anatases and rutiles fall in the ranges 278–392 and 263–264 kJ mol^{-1} respectively, and the activation entropies are all of negative sign. Below 1100 °C, the activation enthalpies are about 714–971 kJ mol^{-1}, and the activation entropies are all of positive sign. Comparison of the amounts of TiN formed at long reaction times with thermodynamic calculations of the equilibrium phase composition at each temperature suggests that the reactant powder bed experiences a nitrogen concentration substantially in excess of the stoichiometric requirement; diffusion of the gas phase into the bed therefore appears not to be the rate-limiting step. The first-order kinetics, and their virtual independence of the physical and chemical properties of the reactants probably reflect the complexity of the reaction sequence.

1. Introduction

In Part I [1] the effect on the formation of TiN from TiO_2 of a number of variables associated with the starting materials was investigated. The results of Part II [2] indicate that the reaction proceeds via a complex sequence of intermediate phases, the slow step apparently being the conversion of Ti_4O_7, the lowest member of the homologous Magneli series, to Ti_3O_5, having a different structure, which then nitrides directly. From a practical viewpoint, the most important information is the temperature dependence of the overall process, and the effect of process variables on this, even though the mechanistic interpretation of kinetic studies will be complicated by the fact that the results will contain temperature dependence contributions from all the stages in the reaction sequence.

In a previous kinetic study of this reaction [3], Samsonov and Polishchuk used 13 mm diameter pressed granules containing the stoichiometric amount of carbon, which were first subjected to reduced pressure to remove trapped air before exposing them to the nitrogen. The formation of pellets, intended to increase contact between the reacted particles, would also inhibit free gas transport to and from the reactants (although this effect was judged to be small [3]), while the lack of excess carbon would be expected to retard further the reaction. Samsonov and Polishchuk [3] conclude that under their experimental conditions, the reaction rate of their TiO_2 (of unspecified crystalline form) is limited by the diffusion of nitrogen gas and CO through the sample compact, in which the pore sizes and shapes were found to be an important factor.

The present studies were made using several different anatase and rutile powder samples containing excess carbon, and the results were analysed in terms of various mechanistic models.

2. Experimental procedure

The four anatase and two rutile samples described in Part I [1] were hand mixed with carbon C8 and Al_2O_3 as the X-ray diffraction (XRD) internal standard, in the weight ratio 1 TiO_2; 1 Al_2O_3; 0.6 C, by dry grinding and brushing through a 150 μm screen. This mixing method was found to be just as effective as a more laborious process of ball milling in ethanol with tungsten carbide balls. Approximately 300 mg sample charges were placed in small alumina boats, settled by tapping, and fired in groups of six in a larger boat, introduced into an electric tube furnace by means of a push rod through a rubber septum. This method was also used to withdraw the samples to the cold zone of the furnace, still under the nitrogen atmosphere (0.1 l min^{-1}). Kinetic experiments were carried out at five temperatures from 1090–1230 °C. After removal from the furnace, the top layer of the sample bed, which could contain material oxidized by contaminants in the firing gas, was removed and discarded. The remaining sample was hand ground for 4 min in an agate mortar and pestle and analysed

0022–2461

by the quantitative XRD method described in Part I [1].

3. Results and discussion

3.1. Kinetics of carbothermal formation of TiN

Typical growth curves of TiN from rutile and anatase are shown in Figs 1 and 2, respectively. The kinetic curves for the two rutiles and four anatases over the temperature range of this work are of identical shape, as shown by Fig. 3, in which all the kinetic data are plotted on a reduced time scale, $t/t_{0.5}$, where $t_{0.5}$ is the time taken for 50% conversion. Following the procedure of Sharp *et al.* [4], the general shape of the present curves was compared with curves predicted by various reaction models. Of these, three classes of curve are clearly distinguishable, representing reaction rates controlled by diffusion, nucleation, and first-order kinetics; the latter are not derived from a physical model, and merely represent a convenient mathematical description of the curves. When the experimental data of Fig. 3 are compared with these three curve shapes (Fig. 4) they conform most closely to the first-order curve. Although the first-order curve shape is also very similar to curves derived from models in which the rate is controlled by the movement of a phase boundary through a disc or sphere, the present results are better described by the first-order equation, especially in the latter stages of the reaction.

The first-order rate equation can be written

$$\log(1 - x) = kt \qquad (1)$$

where x is the degree of reaction at time t and k is the rate constant. The first-order rate constants for all the samples, derived from the slopes of plots of $\log(1 - x)$ against time are shown in Table I. These rate constants were used to construct Arrhenius plots ($\log k$ versus $1/T$) for each of the starting materials, the slopes of which yield the activation enthalpy for the reaction. An alternative procedure for obtaining activation enthalpies without the assumption of a reaction model is to plot $\log(1/t_{0.5})$ versus $1/T$; the results of this approach gave satisfactorily similar results to those derived from the first-order rate law. The Arrhenius plots for both rutile and anatase were composed of two linear portions of different slope,

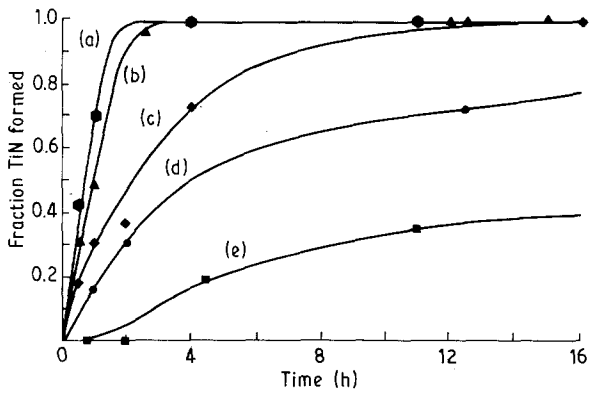

Figure 1 Growth curves of TiN from rutile R1 at (a) 1230 °C, (b) 1200 °C, (c) 1150 °C, (d) 1115 °C, (e) 1090 °C.

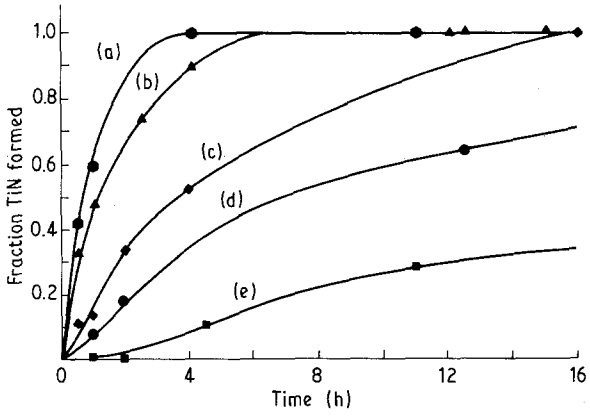

Figure 2 Growth curves of TiN from anatase A1 at (a) 1230 °C, (b) 1200 °C, (c) 1150 °C, (d) 1115 °C, (e) 1090 °C.

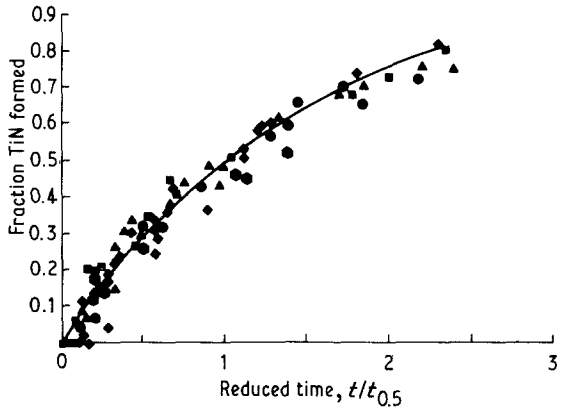

Figure 3 Reduced growth curve for TiN formation, containing data for rutiles R1-2, and anatases A1-4 at all temperatures, superimposed upon a first-order curve.

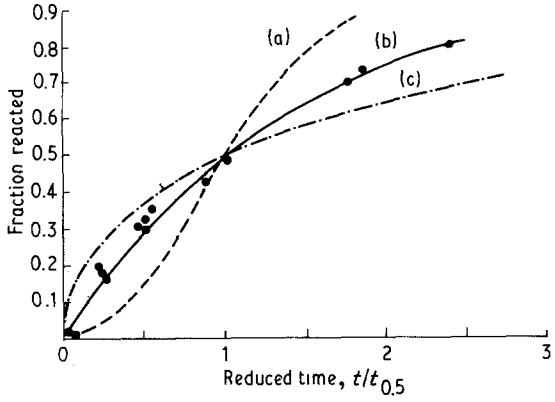

Figure 4 Theoretical growth curves for different rate-controlling processes, with data for TiN growth from rutile R1 superimposed. (a) Nucleation-controlled model, (b) first-order model, (c) diffusion-controlled model.

intersecting at about 1100 °C. In some samples, the two lines were more clearly defined than in others, as illustrated by Figs 5 and 6.

The activation enthalpies for the high temperature region of the Arrhenius plots are collected in Table II, which also contains the activation free energies, ΔG^*, calculated from the expression

$$k = RT/Nh \exp(\Delta G^*/RT) \qquad (2)$$

TABLE I First-order rate constants for carbothermal synthesis of TiN from TiO_2

Sample	Rate constants (10^6 s^{-1})				
	1090 °C	1115 °C	1150 °C	1200 °C	1230 °C
R1	5.90	22.5	38.8	83.3	128.2
R2	0.81	3.78	10.6	23.1	35.5
A1	3.73	11.9	25.6	64.1	138.9
A2	2.43	7.55	20.8	55.6	83.3
A3	2.17	8.17	24.9	55.6	83.3
A4	3.47	14.8	30.3	92.6	128.2

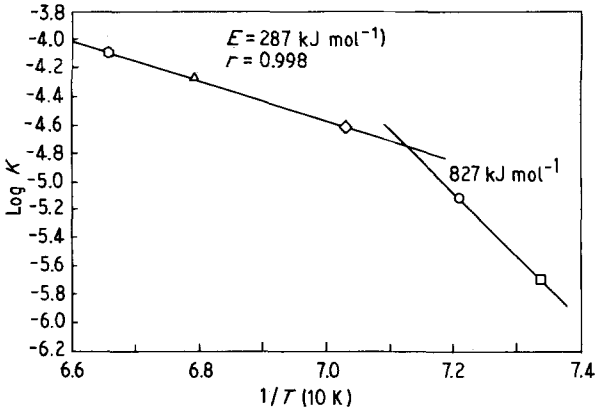

Figure 5 Arrhenius plot for TiN formation from anatase A3, showing clearly the high- and low-temperature processes.

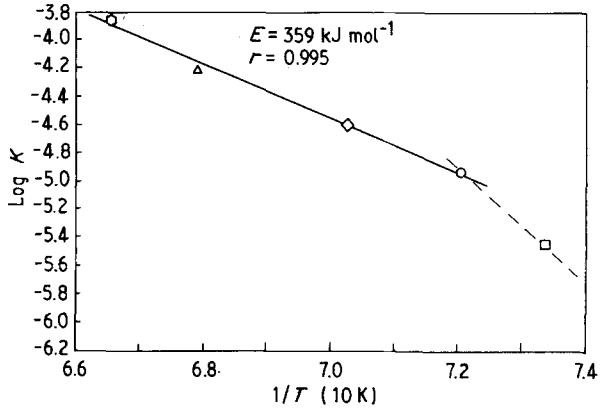

Figure 6 Arrhenius plot for TiN formation from anatase A1, typical of a material in which the two processes are seen less clearly.

and the activation entropy, ΔS^*, calculated from

$$\Delta S^* = (\Delta H^* - \Delta G^*)/T \quad (3)$$

The activation enthalpies of the reaction occurring above 1100 °C have values in the range 263–264 kJ mol^{-1} for rutile and 278–392 kJ mol^{-1} for anatase. The latter values are similar to the activation enthalpies for the transformation of anatase to rutile under hydrogen/nitrogen atmospheres (115 kcal mol^{-1} or 481 kJ mol^{-1} [5]), the products of which, although still retaining the rutile structure, have undergone sufficient reduction to cause a dark grey–blue colouration. These activation enthalpies are very different from the value of 120 kJ mol^{-1} published by Samsonov and Polishchuk [3], whose experimental conditions were, however, significantly different from those

TABLE II Activation thermodynamic functions (> 1100 °C) for carbothermal synthesis of TiN from TiO_2. (Values for 1090 °C calculated by extrapolation using the high-temperature activation enthalpy)

Sample	Temperature (°C)	ΔH^* (kJ mol^{-1})	ΔG^* (kJ mol^{-1})	ΔS^* (J $°C^{-1}$ mol^{-1})
R1	1090	263	489	− 166
	1115	263	483	− 158
	1150	263	489	− 159
	1200	263	497	− 159
	1230	263	502	− 159
R2	1090	264	511	− 182
	1115	264	503	− 172
	1150	264	504	− 169
	1200	264	513	− 169
	1230	264	518	− 169
A1	1090	392	494	− 99
	1115	392	490	− 95
	1150	392	494	− 95
	1200	392	500	− 96
	1230	392	501	− 95
A2	1090	278	499	− 162
	1115	278	495	− 156
	1150	278	496	− 153
	1200	278	502	− 152
	1230	278	507	− 152
A3	1090	287	500	− 157
	1115	287	494	− 150
	1150	287	494	− 146
	1200	287	502	− 146
	1230	287	507	− 147
A4	1090	330	495	− 121
	1115	330	487	− 113
	1150	330	492	− 113
	1200	330	496	− 112
	1230	330	502	− 114

of this work. The activation enthalpies for the reaction below 1100 °C are estimated with less certainty as no less than 714–971 kJ mol^{-1}.

The negative sign of ΔS^* for the high-temperature reaction (Table II) suggests that at these temperatures the product is more ordered than the reactant. Because the activation entropies reflect the relative order (or disorder) of the reactants and products, they should be related to the physical properties of the starting material (providing the product is similarly ordered in each case). The activation entropies were found to correlate well with the surface area of the TiO_2 reactants, calculated from the particle size distribution (Fig. 7), suggesting that increasing surface area is generally a useful indicator of increasing disorder, except in the case of rutile R2.

The ΔS^* values estimated as well as possible for the lower temperature reaction are all highly positive, suggesting that the product of this reaction is highly disordered with respect to the reactant. At the transition point between the two reaction regimes, the ΔS^* values imply that the products undergo abrupt ordering, although this is not reflected in the XRD traces of the TiN formed at these temperatures.

The TiN growth curves at long reaction times also yield information about the maximum amount of TiN likely to be formed at each temperature, which can be compared with thermodynamic calculations of the

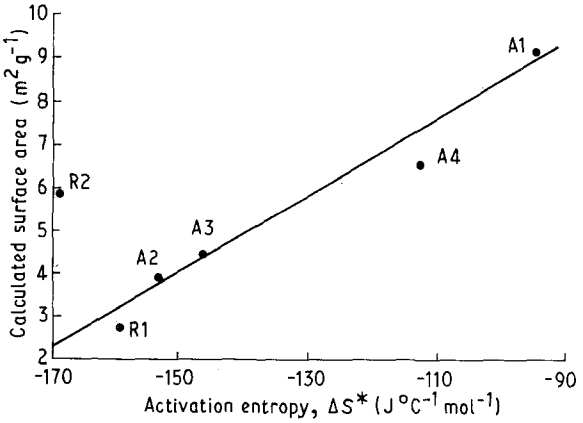

Figure 7 Relationship betweeen the surface areas of the TiO_2 starting materials, calculated from their particle size distribution data, and their activation entropies of TiN formation.

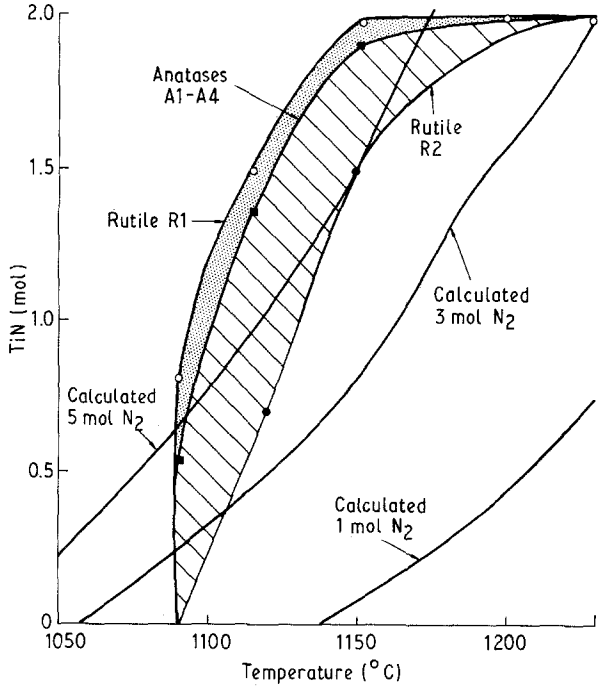

Figure 8 Amount of TiN formed from the rutiles and anatases after 12.5 h reaction, compared with TiN contents calculated by the SOLGASMIX program for various initial nitrogen contents.

equilibrium TiN contents, obtained from the SOLGASMIX program (Part II [2]). For the purpose of the comparison, the measured TiN weight fractions after 12.5 h reaction were read from the kinetic curves and recalculated as molar concentrations produced from 2 mol TiO_2, assuming a constant content of 2 g at Ti. The long reaction time was chosen so that the samples would have the best chance of reaching equilibrium. The results, plotted in Fig. 8, indicate that rutile R1 is the most reactive, achieving maximum TiN content almost 100 °C lower than rutile R2. The various anatase results fall between the two rutiles, and, being similar to each other, were averaged to simplify Fig. 8. For comparison, the phase contents at various temperatures, calculated from thermodynamic considerations for three initial nitrogen concentrations by the SOLGASMIX program are shown in Fig. 8. These curves indicate that as the initial nitrogen concentration is increased, the onset of TiN formation should occur at progressively lower temperatures. The temperature range in which TiN occurred in the present experiments suggests the effective nitrogen atmosphere was close to 5 mol; allowing for the probability that the experimental runs had probably not achieved full equilibrium even after 12.5 h, the equilibrium for the experimental data would lie at even lower temperatures, implying an effective nitrogen content greater than 5 mol in the reaction bed of the dynamic gas flow experiments.

3.2. Mechanism of carbothermal formation of TiN

The reaction sequence established in Part II of this paper [2] suggests two types of reaction

(i) formation of Ti_4O_7 by progressive reduction of TiO_2;

(ii) removal of the final oxygen, with concomitant nitrogen substitution.

Reduction of TiO_2 to its lower oxides may occur either by direct interaction between the carbon and oxygen atoms (contact or direct reduction) or through the gas phase (indirect reduction), or by both processes simultaneously. The two processes can be written

$$TiO_2 + 2C + \tfrac{1}{2}N_2 \rightarrow TiN + 2CO \quad (4)$$

$$TiO_2 + 2CO + \tfrac{1}{2}N_2 \rightarrow TiN + 2CO_2 \quad (5)$$

The free-energy changes for Reactions 4 and 5 at 1127 °C are -153 and $18\,kJ\,mol^{-1}$, respectively. Thus, the lower activation energy for TiN formation found by Samsonov and Polishchuk [3] may be due to a greater predominance of contact reduction in their pressed pellet samples, because any technique which increases contact between the particles should facilitate contact reduction. Although Bogmolov *et al.* [6] observed a faster reaction rate in briquettes, the present work indicated no improvement in reaction rate when the reactants were ball-milled together, suggesting that contact reduction was less significant in these powder samples. The use of more intense mechanical grinding of the reactants has been reported [7] to produce the further complication of mechanochemical formation of carbon–oxygen complexes, which increase the carbon content of the product.

The alternative indirect reduction mechanism occurs through the gas phase, the reducing agent in this case being CO which is formed by reaction of carbon with CO_2 (Equation 5). The initial formation of CO_2 is by reaction with entrapped or surface-adsorbed air in the pores, or as a contaminant in the nitrogen atmosphere. The process occurs by adsorption of CO on to the surface layer of the oxide where combination with the oxygen atoms occurs. The resulting CO_2 molecules are desorbed and regenerated by reaction with the carbon present. Removal of oxygen from the oxide crystal lattice forms vacancies surrounded by especially reactive unsaturated titanium atoms, which attract nitrogen (or carbon) atoms. The resulting

concentration gradient is balanced by diffusion of oxygen out of the bed and nitrogen in, the process continuing until the composition of the particle moves from the homogeneity range of the reactant to that of the product. From this it might be expected that the kinetics would follow a diffusion-controlled rate law, but this was not observed in the present work, suggesting that the diffusional processes involved in indirect reduction are not rate-controlling.

The mean equivalent spherical particle sizes of the present reactants (0.1 μm [1]) were found by TEM to increase on reaction to a maximum of 2 μm, the greatest grain growth occurring during the initial oxide reduction stages. By simple geometry, the pores between close-packed spheres of these sizes are calculated to be 40 and 800 nm, respectively. Thus, the gas flow in the pores of the final product will be much higher than in the original mixture, in which a high partial pressure of CO will occur even close to the surface of the powder bed, retarding the reaction. The subsequent nitridation step involves removal of most of the carbon as CO, resulting in an opening up of the pores, and the movement of the nitridation front from the top of the powder bed to the bottom. Thus, neither the rate of gas flow in the pores of the powder charge nor the particle size of the starting oxides exerts a large influence on the rate of the overall reaction.

4. Conclusions

The formation of TiN from both the anatase and rutile forms of TiO_2 by carbothermal reduction can be described in terms of a first-order kinetic equation. Equations based on diffusion or nucleation models are not appropriate. Arrhenius plots of the first-order rate constants for both the anatases and rutiles consist of two straight lines intersecting at about 1100 °C in all cases. Arrhenius plots based on the initial slopes of the growth curves and independent of a kinetic model give closely similar results. The activation enthalpies for the high-temperature region range from 263–264 kJ mol^{-1} for the rutiles and 278–392 kJ mol^{-1} for the anatases, more than double the value previously reported for pelletized samples containing no excess carbon [3]. These results suggest contact reduction plays a more important role in pellet samples. The activation enthalpies for the low-temperature regions are about 714–971 kJ mol^{-1}. Calculations of the free energies and entropies of activation indicate that above 1100 °C the activation entropies are of negative sign, suggesting that the product is more ordered than the reactant. A correlation between these activation entropies and the surface areas of the starting oxides, estimated from their particle size distributions, suggests that the latter measurements provide a useful indication of the crystalline ordering of the starting oxides (with the exception of rutile R2).

Comparison of the amounts of TiN formed in the kinetic experiments at long reaction times with equilibrium thermodynamic calculations suggests that all the material in the reaction bed is experiencing a nitrogen concentration substantially in excess of the stoichiometric requirement; the rate-limiting factor in the reaction therefore appears not to be the accessibility of the nitrogen to the reactant particles.

The success of the first-order rate law in describing the kinetics is probably a reflection of the complexity of the reaction sequence, which also provides a possible explanation for the fact that the kinetic parameters are virtually independent of the physical or chemical properties of the starting oxides.

References

1. G. V. WHITE, K. J. D. MACKENZIE and J. H. JOHNSTON, *J. Mater. Sci.* **27** (1992) 4287.
2. G. V. WHITE, K. J. D. MACKENZIE, I. W. M. BROWN, M. E. BOWDEN and J. H. JOHNSTON, *ibid.* **27** (1992) 4294.
3. G. V. SAMSONOV and C. S. POLISHCHUK, *J. Appl. Chem. USSR* **46** (1973) 257.
4. J. H. SHARP, G. W. BRINDLEY and B. N. NARAHARIACHAR, *J. Amer. Ceram. Soc.* **49** (1966) 379.
5. K. J. D. MACKENZIE, *Trans. J. Brit. Ceram. Soc.* **74** (1975) 121.
6. G. D. BOGMOLOV, V. D. LYUBIMOV and G. P. SHVEIKIN, *Zh. Prikl. Khim.* **44** (1971) 1205.
7. V. D. LYUBIMOV, T. V. SHESTAKOVA, G. P. SHVEIKIN and S. I. ALYAMOVSKII, *Russ. J. Inorg. Chem.* **22** (1977) 1620.

Received 23 April
and accepted 5 August 1991